Investigation of Internal Deformation of Lithium-ion Battery and Simulation Model for Internal Short Circuit

Shinichi Amano [1)] Hiromichi Ohira [1)] Nobuhiro Matoba [2)] Yasuhito Aoki [2)]

1) JSOL Corporation, 2-18-25, Marunouchi, Naka-ku, Nagoya, Nagoya 460-0002, Japan

E-mail: amano.shinichi@jsol.co.jp, ohira.hiromichi@jsol.co.jp

2) Toray Research Center, Inc., 2-11, Sonoyama 3-chome, Otsu, Shiga 520-8567, Japan

E-mail: nobuhiro.matoba.x9@trc.toray, yasuhito.aoki.s6@trc.toray

ABSTRACT: Fires caused by the thermal runaway of lithium-ion batteries are one of the important issues associated with practical electric vehicles. Thermal runaway and white-smoke generation during impact and/or crushing is often evaluated as part of the safety testing of electric vehicles. Although short circuits are considered to be caused by the contact between positive and negative electrodes, it is difficult to confirm the type of deformation that occurs inside the battery because the battery explodes as a result of short circuits or thermal runaway. This research aims to elucidate the mechanism of internal short circuits by visualizing the internal deformation state when an internal short circuit occurs. First, to investigate the interior of the lithium-ion battery during large deformation, the battery is held and solidified in its deformed state, and the internal deformation is observed using a digital microscope. Observation of a section plane in the deformed state indicates that the aluminum and copper in the current-collector foil are broken in the upper layer. Furthermore, a shear band is confirmed when connecting the points of the broken collector foil. It is presumed that this internal deformation causes contact between the active materials of the positive and negative electrodes and the foil, which causes an internal short circuit. This result is important to explain why battery cells cause internal short circuits when large deformations occur. In addition, to elucidate the mechanism of this shear band, we propose elucidating the internal short-circuit–generation mechanism by constructing a simulation model to reproduce the shear band.

KEY WORDS: lithium-ion battery, internal short circuit, digital microscope, static compression test, shear band, simulation

1. INTRODUCTION

Lithium-ion batteries have high energy densities, making them attractive for a variety of applications ranging from small electronic devices to electric vehicles and airplanes. The safety of lithium-ion batteries is extremely important because of their widespread use in consumer products, including vehicles. Although much is understood about lithium-ion batteries, very few comprehensive computational models exist for predicting internal short circuits and simulating the deformation of these batteries, using a structural approach.

Several studies have been conducted on the internal short circuits in lithium-ion batteries. An ISC cell-level test method was established by M. Keyser *et al.* [1], which could simulate a situation capable of triggering internal short circuits in four types of cells. This method could be used to determine the mechanism of voltage drop caused by each contact target, such as collector-to-collector, cathode-to-collector, collector-to-anode, and cathode-to-anode. A sharp voltage drop was observed when the collectors were in contact with each other, followed by the aluminum to anodes. Therefore, it was understood that internal short circuits were caused by the contact between the cathode and anode, as a result of deformation.

In an observational study of the internal deformation and short circuits, conducted by Chung *et al.* [2], large-format pouch cells were subjected to local indentation, all the way to failure. The post-mortem examination of the failure zones beneath the punches indicated a consistent slant fracture surface angle to the battery plane. This type of behavior could be described by the critical fracture plane theory, according to which the fracture was caused by the shear stress modified by the normal stress. The necessity of developing a model for this behavior was also indicated.

Although many lithium-ion battery simulation models for deformation have been proposed [3, 4], most of them have been developed to reproduce the F–S properties. Several methods have been proposed to model the different properties in the vertical and horizontal directions, also. However, because most of these

methods were developed to predict the conditions before a consistent slant fracture surface was created, they could not represent the internal short-circuit conditions.

In this study, to confirm the deformation state of the internal cells, which causes a short circuit, a laminate of electrodes and separators, without an electrolyte solution, was prepared, subjected to a crush test, and allowed to solidify to visualize the internal deformation state. A simulation model that confirmed the generation of consistent slant fracture surfaces was also developed.

2. EXPERIMENTS

2.1. Specimen for Compression Test

A prismatic automotive battery was disassembled, and the extracted cathode, anode, and separator were washed and restacked to create a model laminated cell. A sample of diameter 34.5 mm and thickness approximately 6 mm was prepared.

2.2. Equipment for Compression Test

A compression test was performed as shown in Fig.1. The indenter was a round bar with a diameter of 10 mm, and it was displaced up to 5 mm at a crosshead speed of 5 mm/min. The load history was measured using a load cell.

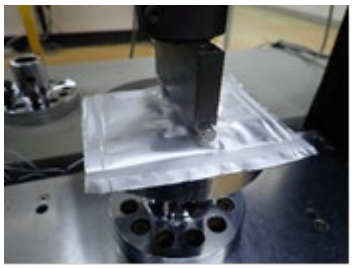

Fig. 1 Specimen and round-bar compression testing equipment.

2.3 Round-bar Compression Test

The force–stroke curve obtained during the mechanical testing is shown in Fig.2. As the first displacement part contains a blank running portion, the curve begins after a displacement of 1.5 mm. A drop in load is observed after reaching a load of 5 kN. The load is sustained in a reduced state for some time, following which it increases again. This reduction in load has been reported in the experimental results of E. Sahraei *et al* [5] also.

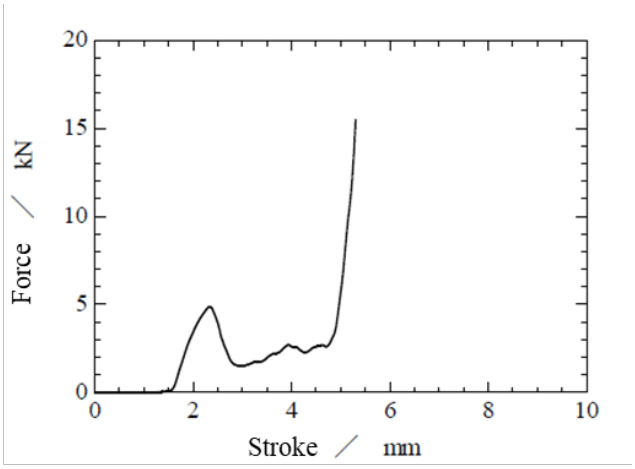

Fig. 2 Force–stroke curve from round-bar compression test.

2.4 Cross Section in Deformed State

Fig.3 shows a digital microscopic photograph of the center cross section of the laminated cell after the deformation test. To observe the deformation state after the first force drop, we performed an additional test to maintain the displacement at 1.87 mm and force at 4.0 kN. A fracture was observed at the center of the cell. In addition, both sides of the cell, which were aligned in the initial state, were misaligned randomly. A detailed observation shows that, while they are not separated by a tear in the middle, each layer has been shifted to the left or right. The central portion of this figure is presented enlarged in Fig.4. The copper foil of the negative-electrode collector and aluminum foil of the positive-electrode collector can be distinguished based on their light brown and silver colors, respectively. The picture shows how they alternately overlap. The top layer of the copper foil does not fracture; however, the lower layers fracture into small fractures. From a macroscopic viewpoint, the shear layer fractures in the inner part of the multilayered laminated cell. Our assumption is that the shear layer generated inside causes the load to escape in the horizontal direction, which generates a random misalignment between the layers, leading to a decrease in the load.

Fig. 3 Cell-center cross section obtained using digital microscope.

Fig. 4 Enlarged view of cell center cross section obtained using digital microscope.

2.5 Flat-plate Compression Test

A flat-plate compression test was performed to determine the compression characteristics of the battery cells. The specimen diameter was 17 mm, height was 10.4 mm, and test speed was 5 mm/min. The flat-plate compression test also produced a decrease in the load, similar to the round-bar compression test. Therefore, the compressive properties of the separator and active material were fitted from the compressive-force–stroke curve.

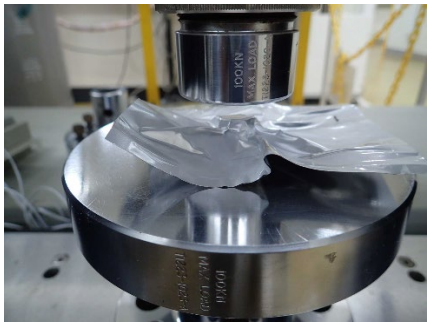

Fig. 5 Specimen and flat-plate compression testing equipment.

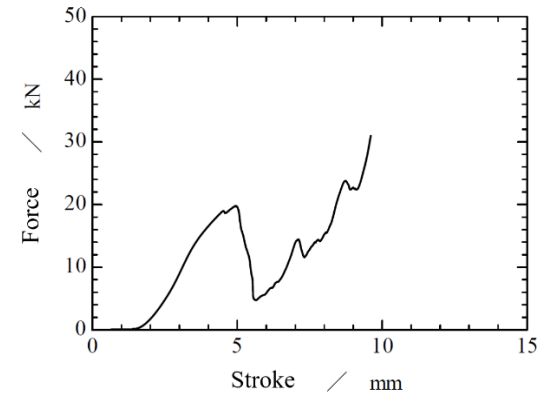

Fig. 6 Force–stroke curve from flat-plate compression test.

2.6. Test Specimen and Details of Tensile Test

A prismatic automotive battery was disassembled, and JIS K6251 No. 3 dumbbell test pieces were punched out in the longitudinal direction of the negative electrode (Cu), positive electrode (Al), and separator, as shown in Fig.7. The measurements were conducted at room temperature (23 ° C) in the atmosphere. A tensile test (test speed = 5.0 mm/min, grip interval = 50 mm) was performed using the crosshead displacement method. An image of the surface of the test piece during the test was acquired using a digital image correlation system, and the Poisson's ratio, Young's modulus, and tensile strength were determined. The mechanical properties obtained from the tensile tests are presented in Appendix A.

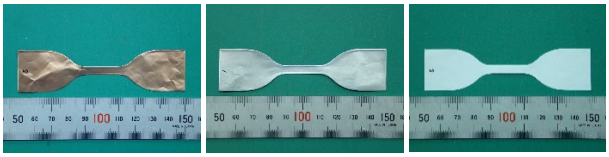

Fig. 7 Typical dumbbell test pieces. Negative electrode (left), positive electrode (center), and separator (right).

3. SIMULATION MODEL

3.1. Model Description

The battery cell modeled in this study consisted of a collector, active material, and separator for the positive and negative electrodes. The active-material layer was present on both the negative and positive-electrode collector sides. The separator was located on the surface of the active-material layer, followed by the active material of the positive electrode, and the collector. This model is illustrated in Fig.8. The green spheres represent the anode active material, orange represents the copper foil, blue represents the separator, red represents the cathode active material, and light blue represents the cathode collector. The separator was modeled using solid elements. The separator was a porous material with different tensile and compressive properties; thus, a honeycomb structure was applied. An elasto-plastic material was applied to the collectors (copper and aluminum) and modeled with shell elements to represent the bending deformation. The active material layer was modeled using DEM elements to reproduce the flow into the separator and collector. The model was created in 2D.

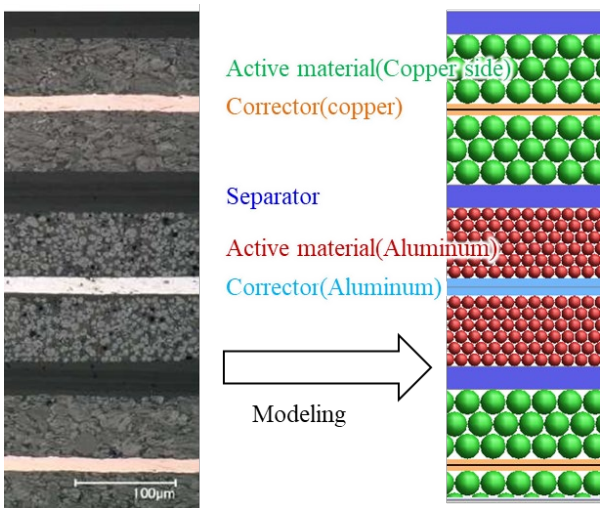

Fig. 8 Simulation model for internal fracture-state reproduction.

3.2. Compression Property Identification

The tensile properties of the collectors of the positive and negative electrodes and separators were determined from the results of the tensile tests. However, the compressive properties of the positive and negative electrodes were largely affected by the compressive properties of the active-material layer. Because the separator was a nonwoven fabric, the tensile and compressive properties were different; therefore, it was necessary to identify the characteristics from the compression test. Each parameter was identified based on the compression test results. Several assumptions were made for identification. First, the compressibility of the active-material layer was identified to be lower than that of the separator, and the compressive properties of the positive- and negative-electrode active-material layers were found to be identical. The compression characteristics of the separator were identified in Section A–B, as shown in Fig.9. Subsequently, the compressive properties of the active material layer in the B–C interval were identified. As shown in Fig.10, the separator was first compressed in Section A–B and then, the compression stiffness was reproduced by embedding the DEM elements of the active-material layer in Section B–C. Penalty stiffness was used to fit the compressive properties of the DEM elements.

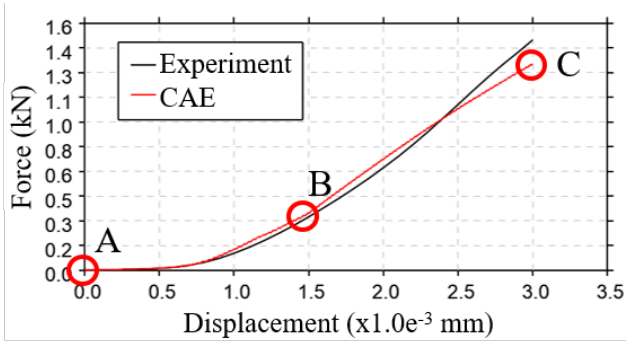

Fig. 9 Compression properties obtained from experiments and CAE.

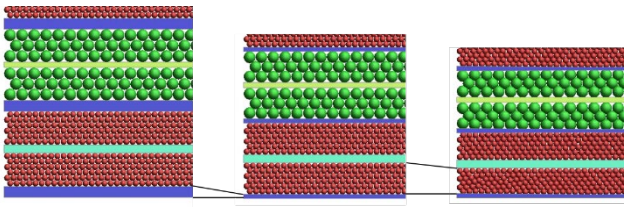

Fig. 10 Compression properties obtained from experiments and CAE.

3.3. Simulation Result

Fig.11 shows the simulation results of battery deformation. First, the aluminum foil layer fractured, which could be because of the weaker tensile strength of the aluminum foil and the localized bending caused by the finer particles. Next, contact occurred between the active materials of the cathode and anode because of the shear band. The active materials were confirmed to be in contact with each other at four points in the shear band. The collectors at the cathode and anode were also close to each other, and it was possible that the collectors are in contact with each other because of element elimination. Fig.12 shows the force–displacement properties of the simulation and test results. The simulation results show a force drop similar to that observed in the test.

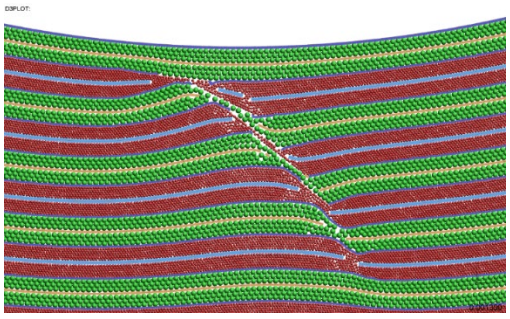

Fig. 11 2D model simulation results

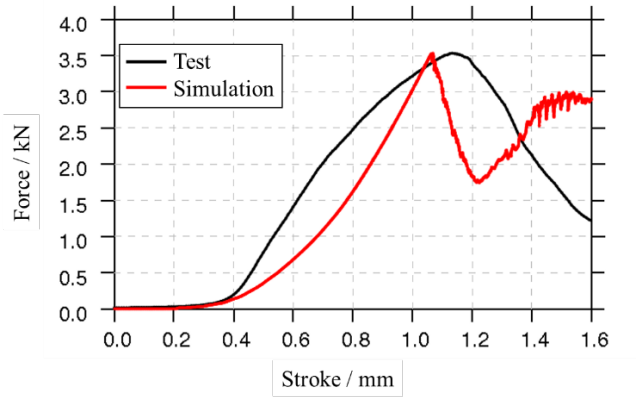

Fig.12 Comparisons between experiments and simulation: Force–stroke curve from static compression test

4. CONCLUSION

In this study, several phenomena that could affect the force–displacement properties of lithium-ion batteries were investigated.

- The deformation inside the laminated cell was observed using a digital microscope photograph of the cell cross section.
- A simulation model was proposed to reproduce the shear band in the active-material layer.
- The simulation results showed a force drop similar to that of the test, owing to the shear band.
- The contact phenomenon between the cathode and anode active-material layers, which was assumed to be the cause of the internal short circuit caused by shear, was observed in the simulation results.

As a future development, we would like to apply SPH or SPG to study the effects of the 3D structure, binder, inhomogeneity of particle arrangement in the active material layer, and particle-size distribution, by applying a constitutive law based on Mohr–Coulomb's fracture criterion for active materials.

ACKNOWLEDGMENT

The authors would like to thank Mr. Nobuhiro Matoba and Mr. Yasuhito Aoki of the Toray Research Center, Inc., for their collaboration with the test program.

REFERENCES

(1) M. Keyser, D. Long, A. Pesaran, E. Darcy, M. Shoesmith, and B. McCarthy, “NREL/NASA Internal Short-Circuit Instigator in Lithium Ion Cells,” NREL/PR-5400-66958 (2015)

(2) S. H. Chung, T. Tancogne-Dejean, J. Zhu, H. Luo, and T. Wierzbicki, “Failure in lithium-ion batteries under transverse indentation loading”, Journal of Power Sources, Volume 389, 15 June 2018, Pages 148-159

(3) S. Schwolow, “Homogenized macro-models of battery packs for crash simulation of electric vehicles,” Automotive CAE Grand Challenge 2021, 19.10.2021

(4) M. Raffler, A. Schmid, F. Feist, and C. Ellersdorfer, “Predictive CAE models of lithium batteries to ensure crash safety of electric vehicles,” Automotive CAE Grand Challenge 2021, 19.10.2021

(5) E. Sahraei, R. Hill, and T. Wierzbicki, “Calibration and finite element simulation of pouch lithium-ion batteries for mechanical integrity,” Journal of Power Sources, 201 (2012) 307– 321

Appendix A : Poisson ratio, Young module, Tensile Strength

[Measurement environment ＝ Room temperature (23 degrees) in air, Test speed = 5.0 mm/min, Chuck distance = 50 mm]

Specimen	Specimen No.	Poisson ratio		Young module / GPa		Tensile Strength / MPa	
		Measurements	Average	Measurements	Average	Measurements	Average
Anode (Cu)	Cu-2	0.336	0.34 (0.02)	81.1	88.2 (5.4)	263	276 (10)
	Cu-3	0.314		90.0		276	
	Cu-4	0.349		87.8		275	
	Cu-5	0.356		93.9		288	
Cathode (Al)	Al-1	0.364	0.32 (0.03)	63.1	61.4 (7.7)	271	272 (1)
	Al-2	0.301		71.5		272	
	Al-4	0.296		57.3		273	
	Al-5	0.304		53.8		272	
Separator	Separator16	0.328	0.30 (0.04)	2.18	2.14 (0.05)		
	Separator17	0.319		2.16			
	Separator18	0.246		2.09			
	Separator2					192	192 (4)
	Separator3					190	
	Separator4					198	
	Separator5					188	

() : Standard deviation